Received: 12 November 2020 | Revised: 16 February 2021 | Accepted: 16 February 2021

DOI: 10.1111/pce.14032

ORIGINAL ARTICLE

Plant, Cell & Environment WILEY

Long-term adaptation of *Arabidopsis thaliana* to far-red light

Chen Hu | Wojciech J. Nawrocki | Roberta Croce

Biophysics of Photosynthesis, Department of Physics and Astronomy, Faculty of Science, Vrije Universiteit Amsterdam, Amsterdam, The Netherlands

Correspondence
Roberta Croce, Biophysics of Photosynthesis, Department of Physics and Astronomy, Faculty of Science, Vrije Universiteit Amsterdam, De Boelelaan 1081, 1081 HV Amsterdam, The Netherlands.
Email: r.croce@vu.nl

Funding information
Nederlandse Organisatie voor Wetenschappelijk Onderzoek

Abstract

Vascular plants use carotenoids and chlorophylls *a* and *b* to harvest solar energy in the visible region (400–700 nm), but they make little use of the far-red (FR) light. Instead, some cyanobacteria have developed the ability to use FR light by redesigning their photosynthetic apparatus and synthesizing red-shifted chlorophylls. Implementing this strategy in plants is considered promising to increase crop yield. To prepare for this, a characterization of the FR light-induced changes in plants is necessary. Here, we explore the behaviour of *Arabidopsis thaliana* upon exposure to FR light by following the changes in morphology, physiology and composition of the photosynthetic complexes. We found that after FR-light treatment, the ratio between the photosystems and their antenna size drastically readjust in an attempt to rebalance the energy input to support electron transfer. Despite a large increase in PSBS accumulation, these adjustments result in strong photoinhibition when FR-adapted plants are exposed to light again. Crucially, FR light-induced changes in the photosynthetic membrane are not the result of senescence, but are a response to the excitation imbalance between the photosystems. This indicates that an increase in the FR absorption by the photosystems should be sufficient for boosting photosynthetic activity in FR light.

KEYWORDS
far-red light acclimation, fluorescence, light harvesting, photosynthesis, photosystems, senescence

1 | INTRODUCTION

Oxygenic photosynthesis is driven by light in the 400–700 nm range (photosynthetically active radiation; PAR). Due to this selective light utilization and shading effect, light is unevenly distributed within a canopy with most of the visible photons being absorbed by the top leaves, while leaves at the bottom receive mainly far-red (FR) light (700–800 nm) (Rivadossi, Zucchelli, Garlaschi, & Jennings, 1999). FR light is of little use for plant photosynthesis because its absorption is limited to a small number of pigments associated with PSI (Croce & van Amerongen, 2013; Santabarbara, Casazza, Belgio, Kaňa, & Prášil, 2020). Indeed, FR light triggers shade-avoidance responses and senescence (Martinez-Garcia et al., 2014).

While the inability to use FR is common to many organisms performing oxygenic photosynthesis, recently, cyanobacteria able to harvest FR photons were reported (Gan, Zhang, et al., 2014). These cyanobacteria redesign their photosynthetic apparatus when exposed to FR light, by synthesizing the FR-absorbing Chlorophylls (Chl) *d* and *f* and integrating them into FR-specific PSI and PSII subunits (Gan, Zhang, et al., 2014; Hu et al., 1998). The newly-assembled FR photosystems effectively use light at wavelengths up to 800 nm (Gan, Shen, & Bryant, 2014; Mascoli, Bersanini, & Croce, 2020; Nurnberg et al., 2018; Soulier, Laremore, & Bryant, 2020), allowing cyanobacteria to grow in dense microbial mats where 'classical' PAR is not available (Chen et al., 2010).

Some algae were also shown to make use of the FR light. Although no eukaryotic algae synthesizing Chl *d* or *f* are known, some

species acclimate to FR light by tuning the absorption of their chlorophylls *a* to lower energy (Kotabova et al., 2014; Wolf & Blankenship, 2019). The integration of these strategies in plants has been proposed as one of the possible ways to increase plant productivity (Blankenship & Chen, 2013). The harvesting of FR photons can be especially relevant in the very crowded crop fields, where only FR light can penetrate (Ort et al., 2015).

In vascular plants, FR light influences the photosynthetic apparatus in several ways on different time scales (Dietzel, Brautigam, & Pfannschmidt, 2008). In the short-term, FR light triggers electron transfer in PSI more efficiently than in PSII resulting in the oxidation of the electron carriers between the two reaction centres (RCs). As a consequence, the major light-harvesting complexes II (LHCII) are dephosphorylated and dissociate from PSI to bind to PSII in a process known as state transitions (Lemeille & Rochaix, 2010). Upon long-term FR acclimation, plants sense the FR light as a low-light trigger and modify their morphology to harvest more photons by elongating their petioles and raising their leaf tips (Franklin & Quail, 2010). The transcript levels in chloroplast genes were found to be regulated under FR-enriched light, showing a lower ratio between PSI (PsaA) and PSII (e.g. PsbB) (Glick, Mccauley, Gruissem, & Melis, 1986). The ratio between PSI and PSII proteins was reported to be lower than that in white light treated leaves (Melis & Harvey, 1981). In agreement with this change in protein composition, the thylakoids showed more and thicker grana than under PAR (Melis & Harvey, 1981). To date, the change in PSI/PSII stoichiometry seems to be the main response of the photosynthetic apparatus of plants to long-term exposure to FR light. However, all the previous studies used a mixture of FR light and light of other wavelengths, mainly red light, which can still be absorbed by both photosystems, although to a different extent. To challenge the plants and see if they are able to develop a stronger response to FR light, here we use light with $\lambda > 700$ nm, which is absorbed only by PSI (Figure S1) and we characterize its effect at the thylakoid level.

It was also reported that both darkness and FR light could promote leaf senescence (Causin, Jauregui, & Barneix, 2006). A recent study showed that extra FR pulses in the dark induce senescence in *Arabidopsis* leaves (Lim et al., 2018), during which gene expression changes and chlorophylls and chloroplast proteins are degraded (Buchanan-Wollaston et al., 2003; Lim, Kim, & Nam, 2007). To investigate whether the FR acclimation is senescence-related, we treated the plants with FR light and we compared their properties with those of plants acclimated to complete darkness.

2 | MATERIALS AND METHODS

2.1 | Plant growth conditions

Wild type (WT) *Arabidopsis thaliana* (Arabidopsis Col-0) were first grown under constant white light (see Figure S1a for the spectrum) at 120 μmol photons/m^2/s, 12 hr/12 hr day/night cycle at 23°C, for 5 weeks. Nutrients were added to the soil only once, before germination. The plants were then separated into three different groups, white light group (WL), far-red light group (FR) and dark group (Dark).

The WL plants were exposed to the same white light conditions as before. FR plants were transferred into a chamber supplied with ~100 μmol m^{-2} s^{-1} FR light (Figure S1a) and grown with 12 hr/12 hr day/ night cycle. The light intensity of FR light was measured using a Laser Power Meter (RoHS, FieldMate). The Dark group was kept in full darkness with the same temperature settings as the WL group.

2.2 | Leaf temperature measurements

A commercial IR thermometer (UT300S) was used for measuring the temperature on the upper and lower face of the leaves. The temperature was read with the light on and the reading on the screen was stable for 5 s. The temperature of each genotype in each growth condition was measured three times on three individual leaves of different plants (Table S1).

2.3 | Chlorophyll fluorescence measurements

The maximum of PSII light use efficiency (F_v/F_m), the PSII efficiency in steady-state in actinic light (Φ_{PSII}) and non-photochemical quenching ($F_m/F_m' - 1$) were measured with a Dual-PAM-100 MODULAR fluorimeter (Walz, Germany) as previously reported (de Bianchi et al., 2011). Measuring light was set at 3 μE, actinic light was 1,024 μmol photons m^{-2} s^{-1} (red) and the red saturating pulse was 4,000 μmol photons m^{-2} s^{-1} for 150 ms. PSII efficiency in steady-state, Φ_{PSII}, was averaged throughout the last 3 min of the 10 min actinic light period.

2.4 | Electron microscopy

The ultrastructure of the chloroplast was imaged by transmission electron microscopy as described in Nicol, Nawrocki, and Croce (2019). The leaves were harvested from the overnight dark-adapted plants, cut into strips and immediately fixed in 0.1 M Caco buffer (pH 7.4) with 2% (v/v) glutaraldehyde and 2% (v/v) paraformaldehyde for 2 hr at room temperature and at 4°C overnight. The fixed leaves were examined and imaged with a JEOL-100CX transmission electron microscope. The number of membrane layer per grana and the grana number per chloroplast were manually counted from the images. The grana and stroma lamella length ratio was obtained using ImageJ software.

2.5 | Thylakoid membranes isolation

Leaves were harvested and kept on ice in the dark or with a dim light and thylakoids were prepared as described previously (Xu, Tian,

Kloz, & Croce, 2015). The isolated thylakoids were suspended in a buffer (20 mM HEPES, pH 7.5, 0.4 M sorbitol, 15 mM NaCl and 5 mM $MgCl_2$), frozen in liquid nitrogen and kept at −80°C until usage.

2.6 | Pigment analysis and leaf chlorophyll content measurements

Chlorophyll *a*/*b* ratio and chlorophyll/carotenoid ratio were obtained by fitting the spectra of the pigment extracts in 80% acetone (measured with a Cary 4000 UV–Vis spectrophotometer) with the spectra of pure pigments according to Croce, Canino, Ros, and Bassi (2002). Chlorophyll concentration was determined using the extinction coefficients reported in Porra, Thompson, and Kriedemann (1989). The relative carotenoid content was obtained by high-performance liquid chromatography analysis according to Croce et al. (2002).

For leaf chlorophyll concentration measurement, a 1 mL pipette tip was used to excise a round piece of the leaf by carefully screwing it on the surface of the leaf. The leaf discs were frozen in liquid nitrogen, crushed in 80% acetone and diluted to an optical density in the chlorophyll Q_y region (about 663 nm) below 1.0.

2.7 | Blue native gels (BN-PAGE) and 2D BN-PAGE

Blue native gels were prepared according to Jarvi, Suorsa, Paakkarinen, and Aro (2011) with the minor modifications described in Bielczynski, Schansker, and Croce (2016). The resolving gels were made with 4–12.5% T (w/v,), 3% C (w/w). The stacking gels were made with 4% (w/v) T and 3% C (w/w), where T is the total concentration of acrylamide and bisacrylamide monomers and C is the relative concentration of the cross-linker bisacrylamide to the total monomer concentration of acrylamide and bisacrylamide.

After running, the blue native gels were cut in strips and loaded onto a Laemmli-SDS-PAGE (Laemmli, 1970) for the second dimension. A 6% T (w/v) acrylamide was used for the stacking gel and 13% T (w/v) for the resolving gel. After running, the gels were stained with a coomassie blue solution (0.1% Coomassie Blue R250 in 10% acetic acid, 40% methanol and 50% H_2O) for 2 hr and de-stained with a de-staining solution (10% acetic acid, 40% methanol and 50% H_2O) for 3 × 2 hr.

2.8 | Immunoblotting

Thylakoids were loaded onto a pre-cast gel [4–12% T (w/v) Bis-Tris Plus, Invitrogen] based on their chlorophyll content. After electrophoresis, the proteins were transferred to a nitrocellulose membrane and stained with Ponceau S solution [0.1% (w/v) Ponceau S in 5% (v/v) acetic acid]. The stained membranes were imaged using a LAS 4000 Image Analyzer (ImageQuant Luminescent) under digital imaging (exposure time: 1/60 s). Afterward, the membranes were blocked with 10% (w/v) milk in TBST (20 mM Tris, pH 7.5, 150 mM NaCl, 0.1% Tween 20) for 1 hr and were incubated with different primary antibodies (all from Agrisera, Sweden) overnight in the dark at 4°C. The primary antibodies included: PsaA (AS06172), PSAG (AS204368), PSAK (AS04049), LHCA1 (AS01005), PsbA (AS10704), PsbC (AS111787), LHCB1 (AS01004), PSBS (AS09533), PetA (AS06119) and ATPC (AS08312). The membranes were washed with TBST for 4× 10 min and then incubated with the secondary antibody (goat anti-rabbit IgG) for another hour. After washing with 4 × 5 min and 2 × 30 min to get rid of the unbound secondary antibody, the membranes were developed for chemiluminescence (SuperSignal West Pico, Thermo Scientific) using a LAS 4000 Image Analyzer. Densitometric analysis of the images was performed using the software ImageJ.

2.9 | Isolation of native protein complexes

The experiments were performed according to Caffarri, Kouril, Kereiche, Boekema, and Croce (2009). The sucrose gradients were produced by freezing a tube containing a sucrose solution (0.5 M sucrose, 20 mM Hepes pH 7.5, 0.06% a-DM) at −80°C and thawing it at 4°C. Samples containing 350 μg Chl were washed with 5 mM EDTA, 10 mM Hepes pH 7.5, diluted to 0.5 mg Chl/ml and then an equal volume of solution for solubilization (1% a-DM in 10 mM Hepes 7.5) was added. The samples were centrifuged at 12,000 × *g* for 10 min and the supernatant was loaded onto the gradients and centrifuged for 16 hr at 4°C at 160,000 × *g*. The bands were collected with a syringe.

2.10 | Low-temperature steady-state fluorescence spectroscopy

Low-temperature steady-state fluorescence emission spectra were recorded using a Fluorolog spectrophotometer. The sample (OD of 0.05/cm at Q_y maximum) was set up in a glass Pasteur pipette inside a transparent Dewar filled with liquid nitrogen. The fluorescence emission spectra were acquired using excitation at 440 nm and recorded with a 1 nm step range from 600 to 800 nm.

2.11 | Room-temperature steady-state absorption spectroscopy

Room-temperature steady-state absorption spectra of sucrose bands were recorded using a Cary 4000 UV–Vis spectrophotometer. The spectra were recorded with a 1 nm step from 350 to 750 nm.

2.12 | Functional PSI/PSII ratio and antenna size measurements in vivo

The ratio of PSI to PSII reaction centres as well as the functional antenna sizes of PSI and PSII were determined by measuring the

electrochromic shift signal (ECS) with a JTS-10 spectrophotometer as described in Nawrocki, Santabarbara, Mosebach, Wollman, and Rappaport (2016). The reaction centre (RC) ratio was measured using a saturating, single turnover flash to trigger charge separation [~630 nm fluorescent dye pumped with a 5 ns full width at half maximum (FWHM) Nd: YAG laser flashes at 532 nm; Minilite II, Continuum] and the detection was done at 520 nm (10 mm thick Schott glass filter, 10 nm FWHM) after subtraction of the signal at 546 nm (10 mm thick Schott glass filter, 10 nm FWHM). The actinic light was prevented from reaching the detector by a 3 mm Schott BG39 filter. The functional antenna sizes were determined using continuous LED light (630 nm, ~300 μmol photons m^{-2} s^{-1}). The initial slope of the ECS rise in light-limiting conditions in a fraction of RCs (i.e. before a single e^- is separated in every RC) represents the maximal, absorption-limited rate of charge separation, which depends—in the absence of acceptor- and donor-side limitations—on the size of antenna functionally connected to the RC. In order to deconvolute the PSI and PSII signals, the leaves were infiltrated with either 10 mM HEPES (pH 7) and 150 mM sorbitol solution (yielding PSII+PSI signal) or with PSII inhibitors (200 μM DCMU and 1 mM hydroxylamine in HEPES-sorbitol; yielding PSI signal only). The quantum yield of PSII $[(F_m - F_0)/F_m]$ was always verified to attain values below 0.05 after the DCMU-HA infiltration to make sure that the inhibition was complete.

3 | RESULTS

3.1 | Plant morphology

Arabidopsis plants were grown in white light (WL) for 5 weeks and then divided into three groups. One group was maintained in WL (WL group), the second exposed to FR light (FR group) and the third kept in the dark (Dark group). Acclimation was followed for 1 week. After 7 days of FR light, the plants displayed extended petioles. Compared with the WL group, the FR-acclimated leaves were smaller and paler, yellowish and faced considerably more upwards (Figure 1). Day 7 Dark plants also raised the tips of the leaves but the yellowing was only observed in older leaves, while younger leaves retained their normal shape and colour (Figure 1). As leaf temperature plays an essential role in the photosystem stability (Mathur, Agrawal, & Jajoo, 2014), to exclude that the observed differences between the WL and FR group were the result of a thermal effect induced by FR-light, leaf temperature was measured on both the upper and lower sides. No FR light-induced heating was observed (Table S1).

3.2 | Photosynthetic parameters

To check how the photosynthetic apparatus acclimates to FR light, maximum PSII efficiency (F_v/F_m), PSII operating efficiency (Φ_{PSII}) and non-photochemical quenching (NPQ) was determined during the treatments (Figures 2 and 3). The WL group showed a relatively stable

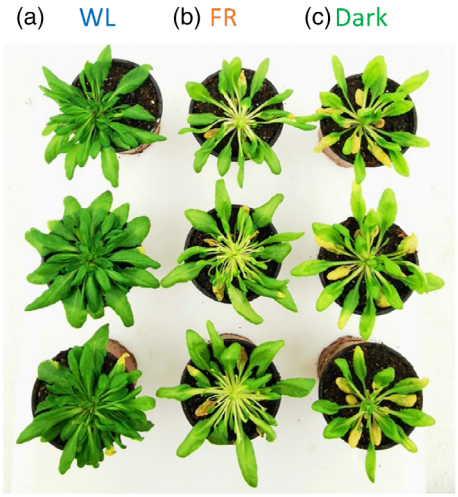

FIGURE 1 Wild type (WT) Arabidopsis plants treated with 7-day with (a) white light (Day 7 WL), (b) far-red (FR) light (Day 7 FR) and (c) dark (Day 7 Dark). Representative plants are shown. The experiment was repeated three times with comparable results

F_v/F_m from Day 1 to 7 (around 0.84), while in both FR and Dark groups the F_v/F_m value decreased after Day 3, reaching 0.77 and 0.57, respectively, after 7 days of acclimation (Figure 2a). Φ_{PSII} was relatively stable from Day 1 to 7 in both Dark and WL group, but 2–3 times lower in the former than in the latter. On the other hand, the Φ_{PSII} of the FR group decreased continuously, reaching 0 at Day 7 (Figure 2b).

After 1 day of treatment, little difference in the NPQ values between WL, FR and Dark group were observed upon red actinic light treatment (Figure 3a), except that the NPQ recovery in darkness was faster in the FR plants than in the other groups. However, from Day 3 to Day 7, the FR group showed a continuous increase in NPQ, with slow induction kinetics and absence of plateau (Figure 3b–d). Moreover, the majority of the fluorescence did not recover when the actinic light was turned off, indicating that photoinhibition occurred during the measurements. After 5 days of FR light, the NPQ signal was almost exclusively due to the non-relaxing component. The behaviour of the FR plants was substantially different from that of the Dark group, in which the NPQ kinetics remained very similar to that of the WL group until Day 5, and only in Day 7 the induction kinetics become slower and the amplitude of NPQ decreased.

3.3 | Structure of the chloroplasts

The ultrastructure of the chloroplasts after 7 days of acclimation was analysed by electron microscopy (Figure 4). Compared with WL and Dark, the FR plants showed an abnormal shape of the chloroplasts (Figure 4a) and the degree of membrane stacking was higher than in the other groups (Figure 4b,c) in agreement with a previous study (Melis & Harvey, 1981); however, the number of grana per chloroplast was lower (Figure 4d). The ratio between grana and stroma lamellae

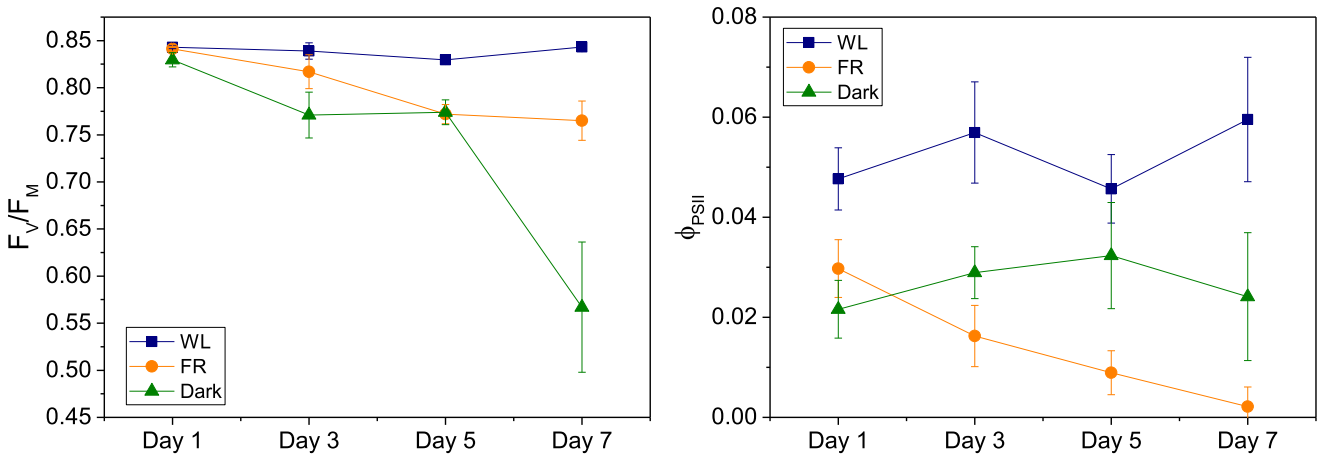

FIGURE 2 F_v/F_m values and PSII efficiency in steady-state in actinic light (Φ_{PSII}) of leaves acclimated to different light conditions from Day 1 to Day 7. Blue squares represent white light (WL), orange circles and green triangles stand for far-red (FR) and dark (Dark) groups, respectively. All data are shown as averages ± *SD* ($n = 3$, biologically independent samples, measured on leaves of a similar age and position in different plants) [Colour figure can be viewed at wileyonlinelibrary.com]

was the highest in FR chloroplast (about two times higher than in WL), and the lowest in Dark chloroplast (Figure 4e).

3.4 | Pigment composition of the thylakoid membranes

Next, we investigated how the leaf chlorophyll content and pigment compositions changed upon acclimation to long-term FR light. Upon 7 days of treatment, the leaf chlorophyll content of both FR (155.0 ± 36.8 μmol/m^2) and Dark (71.7 ± 44.4 μmol/m^2) groups were lower than that of the WL group (252.4 ± 41.5 μmol/m^2, Figure 5a). During the 7 days of treatment, WL plants kept a relatively stable Chl *a*/*b* ratio (3.34 ± 0.17). The Chl *a*/*b* ratio of the FR group instead was already lower than that of the WL group after 1 day of treatment (2.99 ± 0.06) and decreased further throughout the treatment (Figure 5b). The Dark-treated plants showed values similar to that of the WL up to 3 days, followed by an increase to 3.91 ± 0.06 and 3.77 ± 0.06 after 5 and 7 days, respectively (Figure 5b). The Chl/Car ratio in the WL group remained close to the starting value (3.60 ± 0.04) while the ratio dropped in both FR- and Dark- groups during the treatment to 2.65 ± 0.11 and 2.82 ± 0.04, respectively (Figure 5c). The carotenoid composition of the leaves is reported in Figure 5d. After 7-day FR treatment, the relative content of neoxanthin (Nx), violaxanthin (Vx), antheraxanthin (Ax) and lutein (L) increased, while that of β-carotene decreased by 33%. Antheraxanthin (Ax), which was absent in WL, appeared in Day 7 FR plants. Similar to Day 7 FR, Day 7 Dark also showed a higher amount of most carotenoids (relative to Chls) while its β-carotene content was similar to that of the WL group; the de-epoxidation state of the xanthophyll cycle in Day 7 Dark was lower than in Day 7 FR but higher than in Day 7 WL.

3.5 | Protein composition of the thylakoid membranes

To determine the effect of FR acclimation on the composition of the photosynthetic complexes, we analysed the thylakoid composition using native-PAGE and 2D gels (Figures 6 and S3 and Table S2). The proteins were identified on the basis of previous work (Andaluz et al., 2006; Aro et al., 2005; Bielczynski et al., 2016; Caffarri et al., 2009; Takabayashi et al., 2013). After 3 days of acclimation, both FR and Dark plants showed a reduced amount of PSII supercomplexes, PSI-LHCI, PSII dimers and cytochrome b_6f (Cyt. b_6f) as compared to the WL plants. After Day 7 of FR acclimation, we noted a substantial decrease in PSI-LHCI and Cyt. b_6f, but not in the PSII supercomplexes. On the contrary, the content of PSII supercomplex decreased further after 7 days in the dark, while the amount of PSI and Cyt. b_6f remained constant (Figure 6). In conclusion, while FR light induces a strong decrease in PSI, in darkness it is PSII that is degraded first.

To check if the properties of the pigment-protein complexes changed upon FR acclimation, the thylakoids of Day 7 WL and FR plants were solubilized and loaded onto sucrose gradients. Six bands were obtained from both WL and FR thylakoids. Based on their pigment composition, protein composition (Figure 7b), absorption (Figure S4) and fluorescence spectra (Figure 8) and previous results (Xu et al., 2015) they were assigned to: band 1, free pigments; band 2, LHCB monomers; band 3, LHCII trimers; band 4, PSII core (together with some contaminants of proteins that do not contain pigments as the spectrum of band 4 is that of PSII core) c; band 5, PSI-LHCI complexes; band 6 in WL contains mainly PSI in a higher oligomerization state as often observed in sucrose gradients and native gels (Boekema et al., 2001; Heinemeyer, Eubel, Wehmhoner, Jansch, & Braun, 2004; Kouril, van Oosterwijk, Yakushevska, & Boekema, 2005), although a contamination from PSII is also visible both in the gel and in the

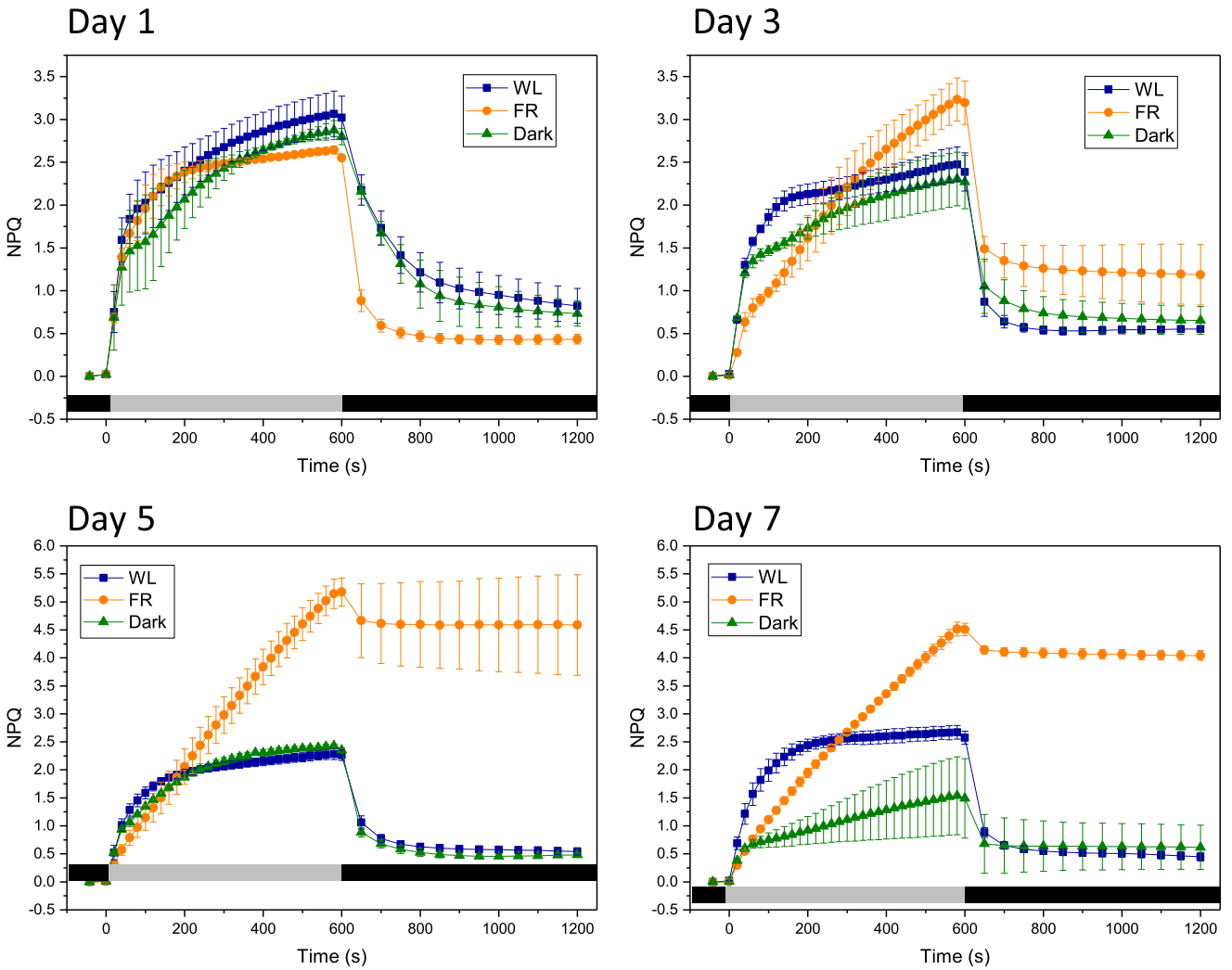

FIGURE 3 Non-photochemical quenching (NPQ) response curves of leaves acclimated to different light conditions for 1–7 days. Blue squares represent white light (WL), orange circles and green triangles stand for far-red (FR) and dark (Dark) groups, respectively. The grey and dark bars on the bottom of each figure represent light/dark periods, respectively. All data are shown as average with ±*SD* ($n = 3$, biologically independent samples, measured on leaves of a similar age and position in different plants) [Colour figure can be viewed at wileyonlinelibrary.com]

spectra. The amount of PSII in band 6 is instead far higher in the FR sample, in agreement with a reduced amount of PSI in these plants. We also observed that the chlorophyll content of bands 5 and 6 from Day 7 FR was significantly lower than that of Day 7 WL (Figure 7a), again in agreement with a lower content of PSI-LHCI in FR (Figure 6). The composition of the other bands was similar between WL and FR membranes.

The properties of the complexes were investigated by low-temperature fluorescence spectroscopy. At 77 K, little differences were observed between the spectra of most complexes from WL and FR, while the spectrum of band 6 reflected the relative increase of PSII supercomplexes in the FR sample (Figure 8). The 77 K fluorescence spectra were also acquired from thylakoids of 3- and 7-day treated plants, confirming this observation (Figure S5). Notably, the emission wavelength of the PSI- and PSII complexes remained unchanged in the FR samples, implying that there were no changes in the red chlorophyll form upon FR acclimation.

3.6 | Functional analysis: PSI/PSII ratio and antenna size of the photosystems

The functional PSI/PSII RC ratio strongly decreased in FR-treated plants with respect to WL plants (Table 1), in agreement with the large decrease in PSI protein level as determined by immunoblots after 7 days of treatment (Figure S6). An increase in PSII functional antenna size and a decrease in PSI antenna size occur during the FR treatment (Table 1). Furthermore, the blots revealed that the Cyt. *f* content (per chlorophyll basis) significantly decreased, while PSBS was up-regulated after FR treatment.

4 | DISCUSSION

In this work, we studied the acclimation of the photosynthetic apparatus of *A. thaliana* to far-red light. Differently from previous studies

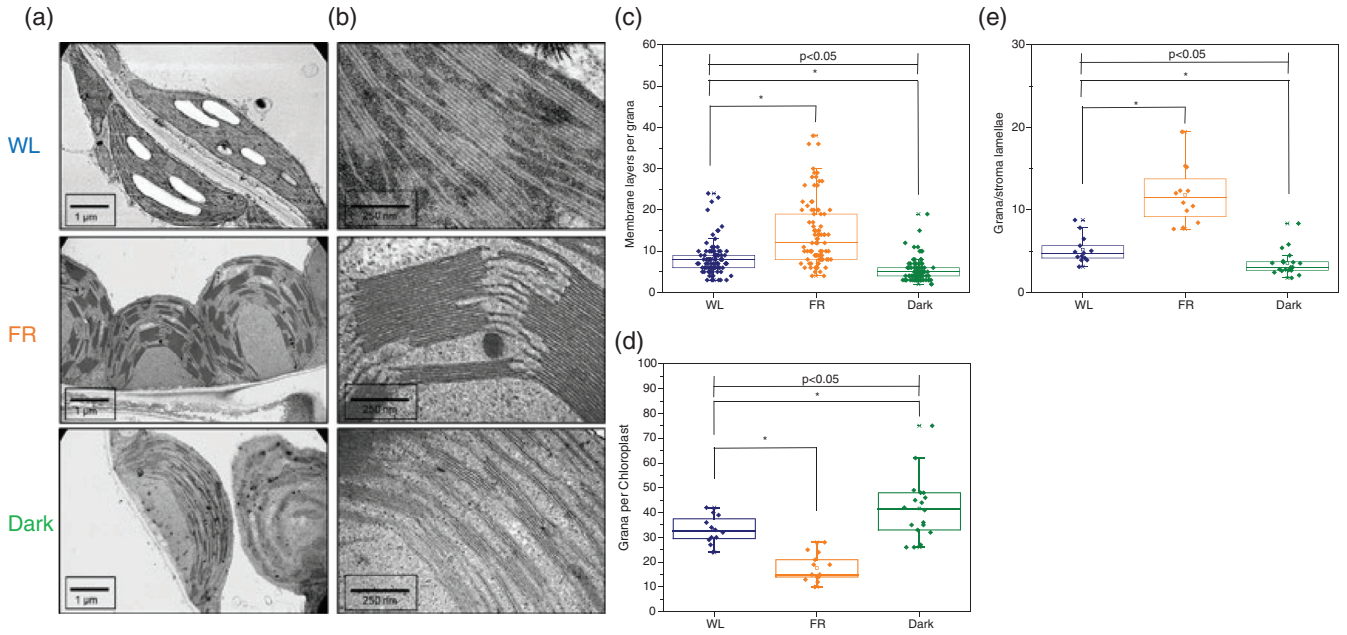

FIGURE 4 (a,b) Representative electron microscopy images of chloroplasts from Day 7 WL (WL), far-red (FR) and dark (dark). (c) Number of membrane layers per grana in each sample ± *SD* ($n > 80$). (d) Grana number per chloroplast in each sample ± *SD* ($n > 10$). (e) Ratio between grana and stroma lamellae ±*SD* ($n > 10$). Blue diamonds represent WL, orange and green diamonds stand for FR and Dark, respectively. The lines in the middle of boxes represent mean values of the samples, box borders and whiskers stand for ±*SE* and ±*SD*, respectively. '*' represents the mean difference (MD) between two groups is statistically significant ($p < .05$, *t* test) [Colour figure can be viewed at wileyonlinelibrary.com]

that used a mixture of red and FR light (Chow, Melis, & Anderson, 1990; Glick et al., 1986; Hogewoning et al., 2012; Kim, Glick, & Melis, 1993; Melis & Harvey, 1981; Walters & Horton, 1994), we treated the plants with pure FR light with $\lambda > 700$ nm. Our goal was to challenge the photosynthetic apparatus as these wavelengths are absorbed almost exclusively by Photosystem I. We also used high-intensity FR light to distinguish the effects of FR acclimation from those of dark-induced senescence, due to a low photon flux.

While, when exposed to FR light, some cyanobacteria synthesize chlorophylls *d* and *f*, enhancing the absorption in the FR region (Gan, Zhang, et al., 2014; Mascoli et al., 2020; Nurnberg et al., 2018), no vascular plants that produce these chlorophylls are known. However, plants do use a small part of the FR light thanks to the so-called PSI red chlorophyll forms, which absorb at wavelengths longer than >700 nm and originate from strongly coupled Chl *a* pigments (Croce & van Amerongen, 2013). The energy and number of red forms differ in different organisms (Gobets & van Grondelle, 2001) and also between plant species (Chukhutsina, Liu, Xu, & Croce, 2020). One of the possible effects of FR acclimation could thus be a change in the red form content as it is the case in some algae (Santabarbara et al., 2020). However, our data clearly show that this is not the case, because the absorption and emission spectra of the individual complexes do not change upon FR treatment (Figures S4 and 8). On the contrary, *A. thaliana* plants exposed to FR light decreased the absolute content of red forms by drastically reducing the amount of PSI. Indeed, the main effect of FR acclimation in Arabidopsis is a substantial decrease in PSI/PSII ratio accompanied by an increase in the PSII antenna size and a reduction in the PSI antenna size (Table 1).

What drives the redesign of the photosynthetic apparatus during FR treatment? In photosynthetic linear electron flow, the two photosystems work in series, with PSII electron transfer rate (ETR) identical to PSI ETR at steady-state. Any changes in light quality (such as an increase in the proportion of the FR in the incident light) or photosystem absorption capacity will temporarily unbalance the electron flow. Photosynthesis has developed multiple mechanisms to counteract the effects of uneven ETRs (reviewed in Chow et al., 1990; Dietzel et al., 2008). Notably, during the short-term relative increase in the FR light, state transitions are employed to balance the excitation and increase the PSII antenna size at the expense of the PSI cross section (Lemeille & Rochaix, 2010; Minagawa, 2011; Mukherjee, 2020; Ruban & Johnson, 2009). Nonetheless, cyclic electron flow, NPQ and water-to-water cycles, as well as long-term acclimation resulting in antennae synthesis or degradation, all have a role in the optimization of unbalanced photosynthetic electron flow (Dietzel et al., 2008). In our experiments, the extreme effect of the FR light, which triggers *only* PSI, leads to the degradation of this complex and an increase of the PSII antenna size in a bid to even PSII and PSI ETRs (Table 1). In line with this, the thylakoid membranes of FR-treated plants become more stacked (Figure 4), increasing the area of the grana (where most PSII locate) as reported before (Melis & Harvey, 1981). Changes in PSI/PSII RC stoichiometry due to changes in light quality are well-documented from cyanobacteria to vascular plants (Fujita & Murakami, 1987; Glick, Mccauley, & Melis, 1985; Melis & Brown, 1980; Shimakawa & Miyake, 2019; Wilhelm, Krámer, & Wild, 1985). We note that this compensation strategy works not only under FR light but also in other conditions that cause

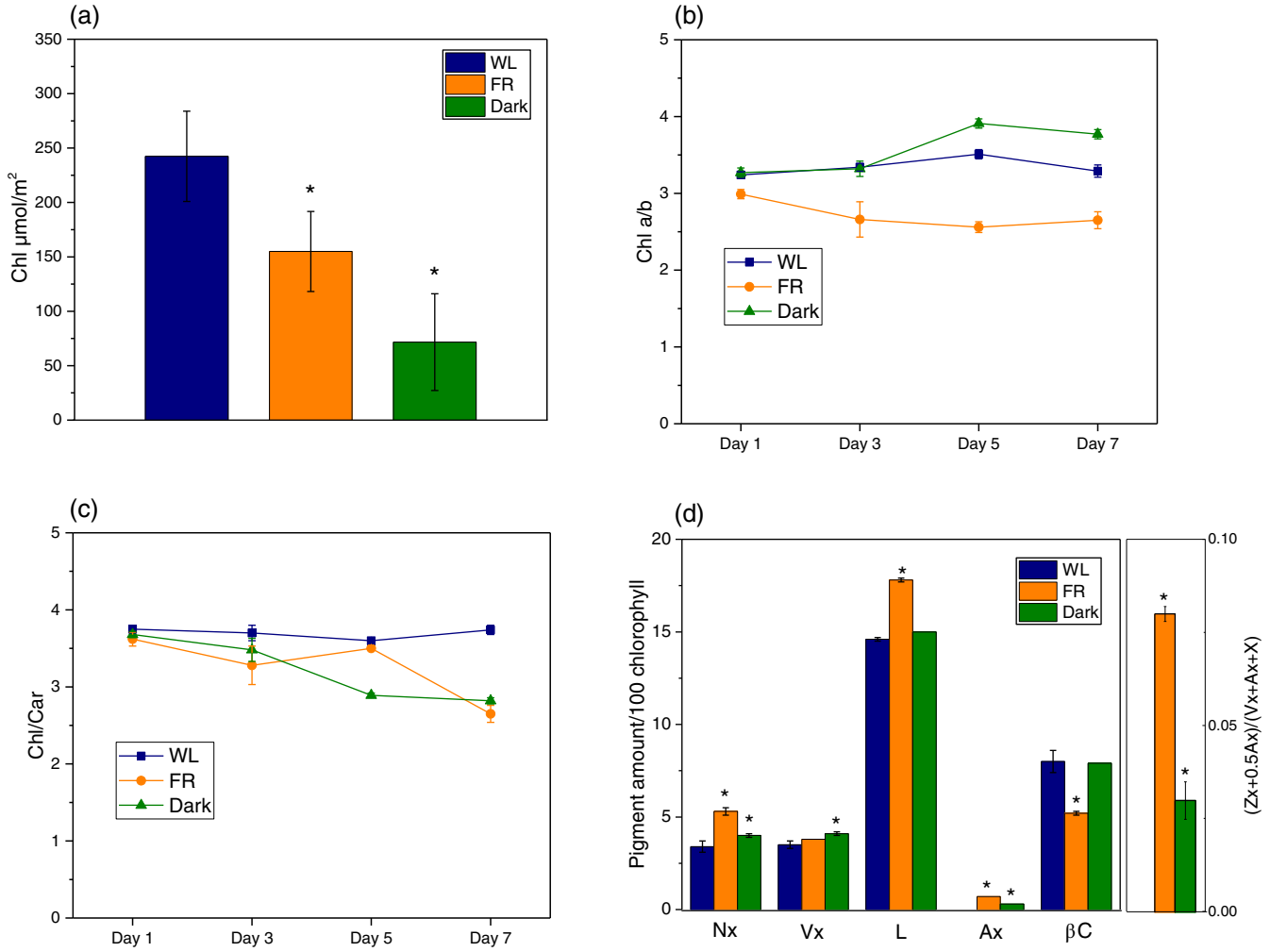

FIGURE 5 Pigment content of leaves and pigment compositions of isolated thylakoids during acclimation. (a) Chlorophyll content of the leaves, (b) Chlorophyll a/b and (c) Chlorophyll/carotenoid ratio of the thylakoids. All data are shown as means ±*SD* ($n = 3$, biologically independent samples). (d) HPLC analysis on carotenoid composition in thylakoid from Day 7 WL, Day 7 far-red (FR) or Day 7 Dark. Neoxanthin (Nx), violaxanthin (Vx), lutein (L), antheraxanthin (Ax), β-carotene (βC) and chlorophylls (Chl a and Chl b). All data are shown as average with ±*SD* ($n = 3$). '*' represents the mean difference (MD) between WL and other groups is statistically significant ($p < .05$, *t* test, $n > 5$). The data are shown in Figure S2. Blue bars and squares represent WL plants, orange bars and circles and green bars and triangles stand for FR- and dark-treated samples, respectively [Colour figure can be viewed at wileyonlinelibrary.com]

the unbalanced PSI and PSII ETRs. Several chlorophyll *b*-deficient mutants of vascular plants show a lower PSI/PSII ratio than their WTs, compensating for a lower excitation level in PSII caused by a small PSII antenna size (Brestic et al., 2015; Kim et al., 1993). Recently, we have also shown that genetic modifications resulting in a decrease of PSII absorption capacity are a trigger to increase the number of PSII RCs to balance the ETRs (Chukhutsina et al., 2020; Nicol et al., 2019).

4.1 | PSII undergoes photoinhibition under actinic light after long-term FR treatment due to a downstream electron transfer bottleneck

Because FR light is enriched in shaded environments, one might expect that plants exposed to FR prepare their NPQ machinery to get ready for sun flecks (Aspinall-O'Dea et al., 2002; Li et al., 2000; Peterson & Havir, 2000). This is particularly important because an increase of PSII/PSI ETR ratio (which is what would occur if the FR acclimated plants are exposed to full sunlight spectrum) is far more detrimental to the photosynthetic organisms than its decrease—the latter mostly resulting in a decrease of efficiency rather than an overreduction of the ETC and ROS production. In line with this, we observed that both the PSBS content (Figure S6) and the xanthophyll de-epoxidation levels increased (Figure 5d) during FR treatment. However, the NPQ value of the FR-treated plant was comparable with that of the WL and Dark groups after the first day and third day of treatment (Figure 3a,b) and strong PSII photoinhibition was observed after exposure of 5- and 7-day FR- treated plants to actinic light (Figure 3c,d). What are the reasons behind this PSII photoinhibition? We exclude the possibility that the FR treatment itself results in PSII damage. This

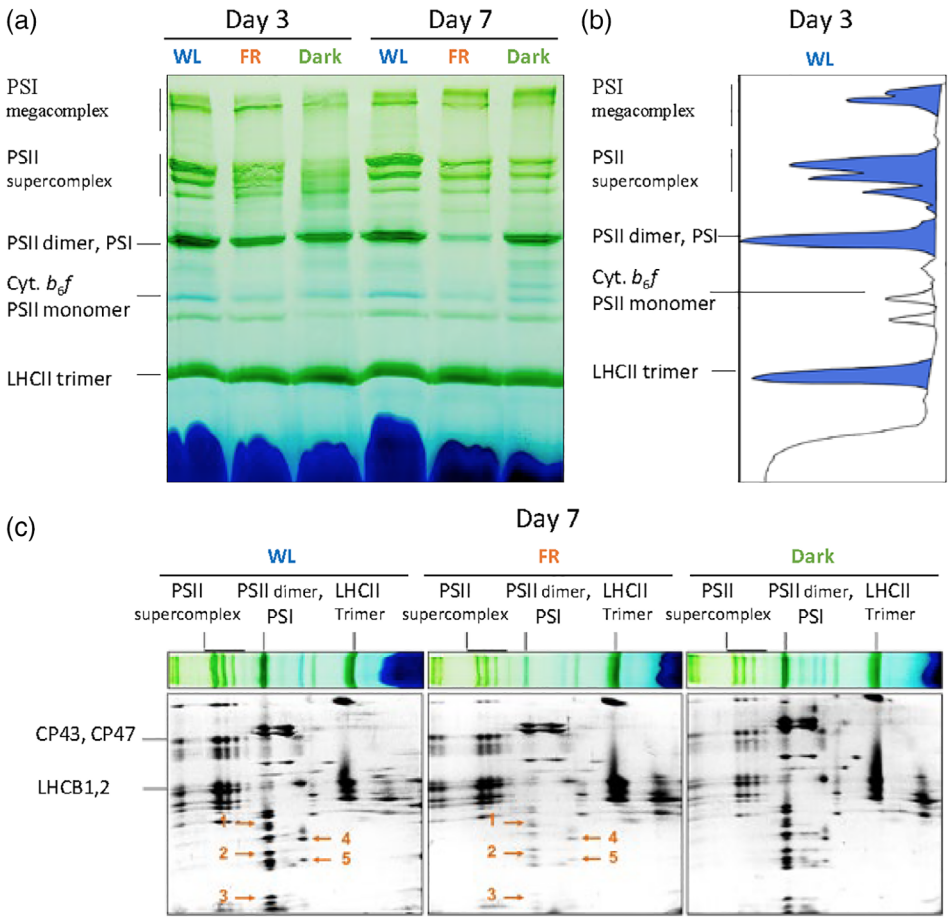

FIGURE 6 Thylakoids composition analysed by 2D BN-PAGE. (a) Blue native gels of thylakoids from 3 or 7 days-treated WL, far-red (FR) and Dark-treated plants. A total of 8 μg of chls were loaded in each lane. (b) Densitometric profile of the bands from Day 3 WL sample (Table S2). (c) Second dimension SDS-PAGE of the blue native gels in Day 7. From left to right: WL, FR and Dark. Orange arrows indicate the following proteins: 1, LHCA3/LHCA2/PSAD; 2, PSAF/PSAL/PSAE/PSAH; 3, PSAG/PsaC/PSAK; 4,5 Cyt. b_6f subunits; as previously reported (Grebe et al., 2019) [Colour figure can be viewed at wileyonlinelibrary.com]

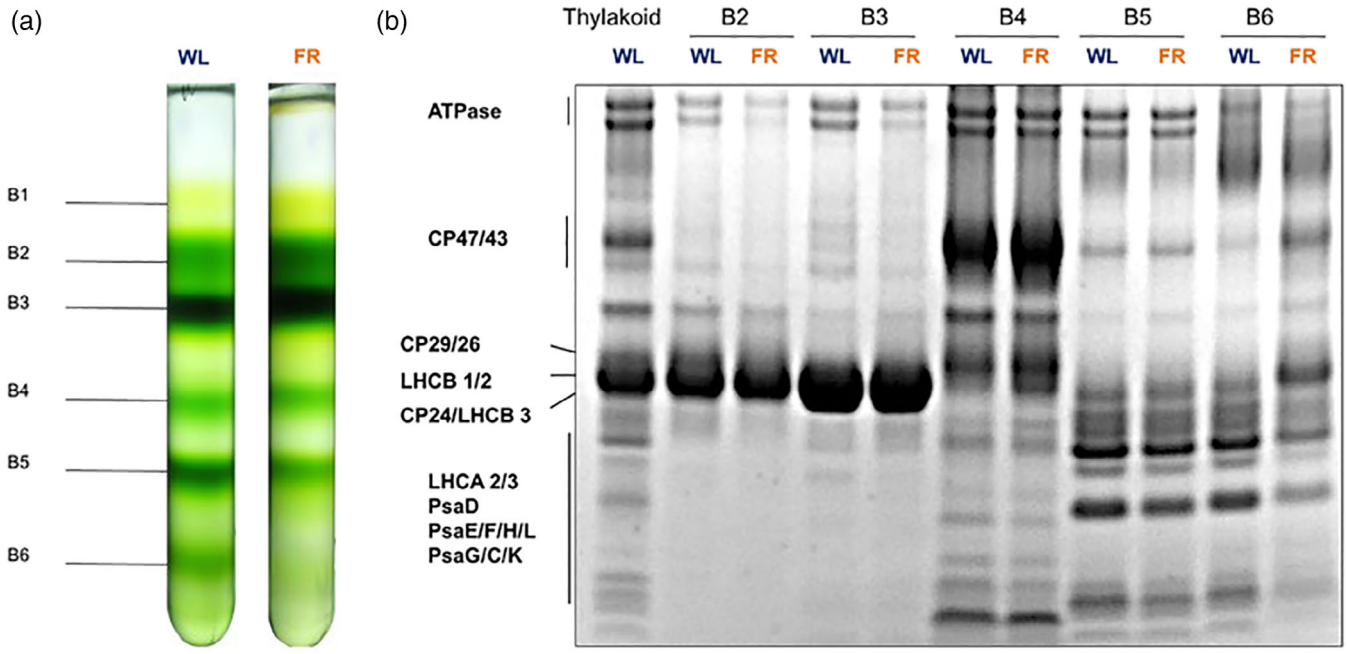

FIGURE 7 Isolation of photosynthetic complexes. (a) Sucrose density gradients loaded with solubilized thylakoid membranes isolated from 7-day white light acclimated (left; WL) and far-red (FR) acclimated plants (right; FR). A total of 350 μg of Chl were loaded in each gradient. (b) Coomassie-stained SDS-PAGE showing the protein composition of the bands from the sucrose gradients. The proteins indicated by arrows were identified based on previous works (Dikaios et al., 2019; Nicol et al., 2019; Suorsa et al., 2014; Wood et al., 2018) [Colour figure can be viewed at wileyonlinelibrary.com]

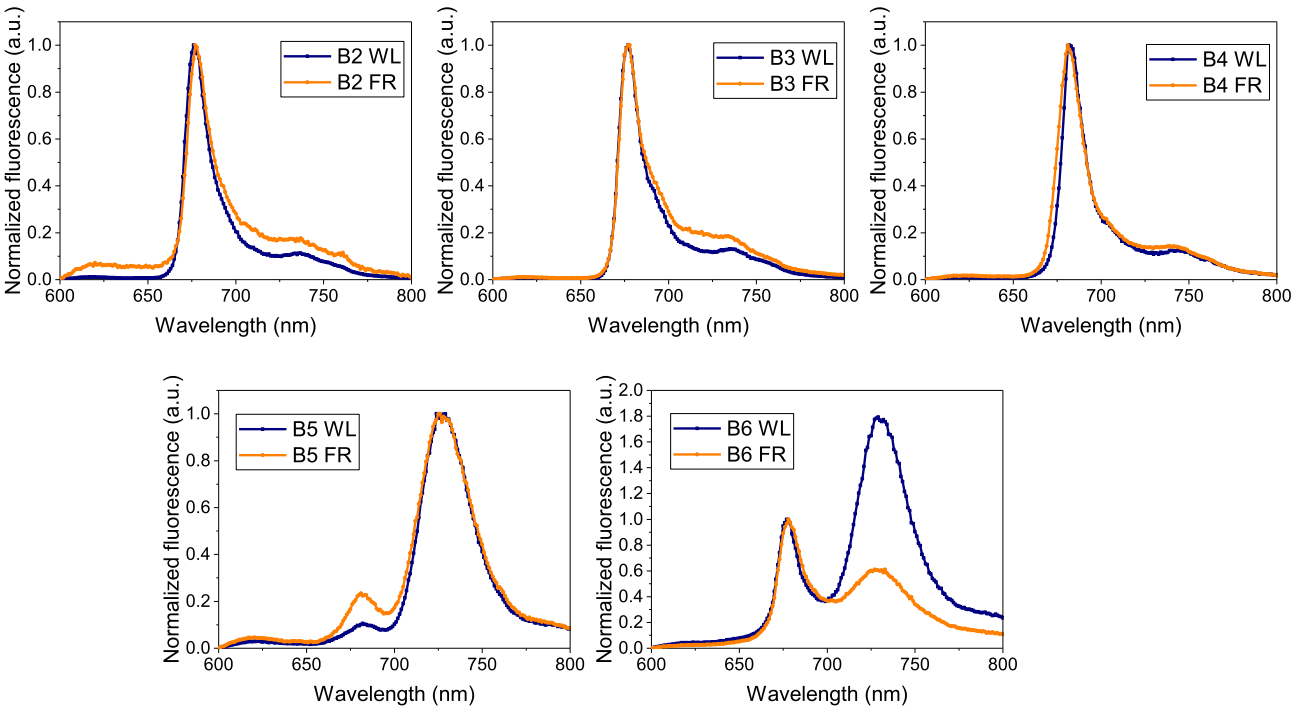

FIGURE 8 Fluorescence emission spectra at low temperature (77 K) from band (B)2 to band 6 isolated by sucrose gradient. The samples from Day 7 WL and Day 7 far-red (FR) are in blue and orange, respectively. The excitation wavelength is 440 nm [Colour figure can be viewed at wileyonlinelibrary.com]

TABLE 1 PSI and PSII content and functional analysis of the Arabidopsis leaves

	WL	FR
Functional analysis		
PSI/PSII RC ratio	0.65 ± 0.05	0.20 ± 0.05*
PSI antenna size	1.00 ± 0.12	0.43 ± 0.09*
PSII antenna size (both relative values)	1.43 ± 0.14	1.64 ± 0.20

Note: RC ratio and antenna sizes of both photosystems measured in vivo using the electrochromic probe. All functional antenna sizes are normalized to the PSI antenna size in WL. All data are means ± *SD* ($n = 5$, biological replicates).
*Mean difference between FR and WL is significant within one group ($p < .05$, *t* test, $n = 3$).

can be theoretically predicted as the spectrum of the FR light does not sensitize the chlorophylls of PSII (Figure S1). Furthermore, F_v/F_m measurements, a proxy for PSII photoinhibition, indicate that PSII remains largely functional even after 7-day FR treatment prior to actinic light exposure (F_v/F_m 0.77 compared to 0.84 in the 7-day WL conditions). The difference in F_v/F_m can be, at least in part, due to the larger antenna size of PSII in FR, which influences the efficiency of the delivery of the excitation to the reaction centre (Wientjes, van Amerongen, & Croce, 2013). Interestingly, dark treatment has a more detrimental effect on PSII than FR light, with F_v/F_m decreasing to 0.57 after 7 days. We then suggest that the rapid, actinic light-induced q_I quenching results from acceptor-side PSII photoinhibition due to the downstream electron transfer bottleneck that can be seen from a decreased Φ_{PSII} (Figure 2b), and that is due to the reduction of PSI and Cyt. b_6f complexes (relative to PSII) (Figures 6 and S6). This indicates that the observed increase of both PSBS and de-epoxidated xanthophylls is not sufficient to protect the cells in these conditions.

4.2 | Long-term FR light effects differ from dark-induced senescence

Senescence is an important strategy for plants adapting to exogenous and endogenous factors to redistribute nutrients and secure the reproductive process (Woo, Kim, Nam, & Lim, 2013). During senescence, leaves become yellow, chlorophyll content decreases and photosynthetic proteins and lipids are degraded (Lim et al., 2007). It is reported that both darkness and FR light can lead to leaf senescence (Brouwer, Ziolkowska, Bagard, Keech, & Gardestrom, 2012; Causin et al., 2006; Degreef, Butler, Roth, & Frederic, 1971; Mishra & Pradhan, 1973), and that extra FR pulses between dark periods can even promote senescence in detached *Arabidopsis* leaves (Lim et al., 2018). In this work, by using high-intensity FR light we were able to disentangle the contribution of the light spectrum- and intensity on the induction of senescence. We found that yellowing of the leaves occurs upon both dark- and FR treatments,

concomitant with a decrease in the Chl content and an increase in Car/Chl ratio, all indications of senescence (Lim et al., 2018). However, the chlorophyll composition of FR- and Dark-thylakoids changed in different directions: the FR group showed a lower Chl *a*/*b* ratio whereas the Dark group showed an increase in the ratio as compared to WL plants. This difference arises as a consequence of the PSI loss upon FR treatment (Figure S6), a finding contrasting with the effect observed during senescence (Kotakis, Kyzeridou, & Manetas, 2014), with PSI being more stable than PSII (Choe & Thimann, 1977).

5 | CONCLUSIONS

In this work, we showed that the plant adaptation strategies to darkness and to intense FR-light are substantially different. In both cases, the shade avoidance response is triggered, together with an increase in the PSII antenna/RC ratio. However, FR-light mediated exclusive sensitization of PSI results in an unbalance of PSII and PSI ETRs, which the plant tries to prevent by degrading PSI. It would be interesting to investigate whether the FR light-acclimated plants could be a model for PSII photoinhibition studies, particularly when exposed to fluctuating light or medium high light—an excess of PSII-borne electrons are blocked due to the bottleneck in the down-stream of ETC. This suggests that the potential for crop yield increase if the plants are engineered to be able to synthesize red-shifted Chlorophylls and extend the range of absorbed light (Allakhverdiev et al., 2016; Nurnberg et al., 2018), could be achieved with rewiring photosynthesis.

ACKNOWLEDGMENTS

We thank Rien Dekker (VU) for help with the EM. This project was supported by the Dutch Organization for Scientific Research (NWO) via a TOP grant to Roberta Croce.

CONFLICT OF INTEREST

The authors declare no conflicts of interest.

DATA AVAILABILITY STATEMENT

The data that support the findings of this study are available from the corresponding author upon reasonable request.

ORCID

Wojciech J. Nawrocki https://orcid.org/0000-0001-5124-3000
Roberta Croce https://orcid.org/0000-0003-3469-834X

REFERENCES

Allakhverdiev, S. I., Kreslavski, V. D., Zharmukhamedov, S. K., Voloshin, R. A., Korol'kova, D. V., Tomo, T., & Shen, J. R. (2016). Chlorophylls *d* and *f* and their role in primary photosynthetic processes of cyanobacteria. *Biochemistry (Mosc)*, *81*(3), 201–212.

Andaluz, S., Lopez-Millan, A. F., De las Rivas, J., Aro, E. M., Abadia, J., & Abadia, A. (2006). Proteomic profiles of thylakoid membranes and changes in response to iron deficiency. *Photosynthesis Research*, *89*(2–3), 141–155.

Aro, E. M., Suorsa, M., Rokka, A., Allahverdiyeva, Y., Paakkarinen, V., Saleem, A., … Rintamaki, E. (2005). Dynamics of photosystem II: A proteomic approach to thylakoid protein complexes. *Journal of Experimental Botany*, *56*(411), 347–356.

Aspinall-O'Dea, M., Wentworth, M., Pascal, A., Robert, B., Ruban, A., & Horton, P. (2002). In vitro reconstitution of the activated zeaxanthin state associated with energy dissipation in plants. *Proceedings of the National Academy of Sciences of the United States of America*, *99*(25), 16331–16335.

Bielczynski, L. W., Schansker, G., & Croce, R. (2016). Effect of light acclimation on the organization of photosystem II super- and supercomplexes in *Arabidopsis thaliana*. *Frontiers in Plant Science*, *7*, 105.

Blankenship, R. E., & Chen, M. (2013). Spectral expansion and antenna reduction can enhance photosynthesis for energy production. *Current Opinion in Chemical Biology*, *17*(3), 457–461.

Boekema, E. J., Jensen, P. E., Schlodder, E., van Breemen, J. F., van Roon, H., Scheller, H. V., & Dekker, J. P. (2001). Green plant photosystem I binds light-harvesting complex I on one side of the complex. *Biochemistry*, *40*(4), 1029–1036.

Brestic, M., Zivcak, M., Kunderlikova, K., Sytar, O., Shao, H., Kalaji, H. M., & Allakhverdiev, S. I. (2015). Low PSI content limits the photoprotection of PSI and PSII in early growth stages of chlorophyll *b*-deficient wheat mutant lines. *Photosynthesis Research*, *125*(1–2), 151–166.

Brouwer, B., Ziolkowska, A., Bagard, M., Keech, O., & Gardestrom, P. (2012). The impact of light intensity on shade-induced leaf senescence. *Plant Cell and Environment*, *35*(6), 1084–1098.

Buchanan-Wollaston, V., Earl, S., Harrison, E., Mathas, E., Navabpour, S., Page, T., & Pink, D. (2003). The molecular analysis of leaf senescence – A genomics approach. *Plant Biotechnology Journal*, *1*(1), 3–22.

Caffarri, S., Kouril, R., Kereiche, S., Boekema, E. J., & Croce, R. (2009). Functional architecture of higher plant photosystem II supercomplexes. *EMBO Journal*, *28*(19), 3052–3063.

Causin, H. F., Jauregui, R. N., & Barneix, A. J. (2006). The effect of light spectral quality on leaf senescence and oxidative stress in wheat. *Plant Science*, *171*(1), 24–33.

Chen, M., Schliep, M., Willows, R. D., Cai, Z. L., Neilan, B. A., & Scheer, H. (2010). A red-shifted chlorophyll. *Science*, *329*(5997), 1318–1319.

Choe, H. T., & Thimann, K. V. (1977). The retention of photosynthetic activity by senescing chloroplasts of oat leaves. *Planta*, *135*(2), 101–107.

Chow, W. S., Melis, A., & Anderson, J. M. (1990). Adjustments of photosystem stoichiometry in chloroplasts improve the quantum efficiency of photosynthesis. *Proceedings of the National Academy of Sciences of the United States of America*, *87*(19), 7502–7506.

Chukhutsina, V. U., Liu, X., Xu, P., & Croce, R. (2020). Light-harvesting complex II is an antenna of photosystem I in dark-adapted plants. *Nature Plants*, *6*, 860–868.

Croce, R., Canino, G., Ros, F., & Bassi, R. (2002). Chromophore organization in the higher-plant photosystem II antenna protein CP26. *Biochemistry*, *41*(23), 7334–7343.

Croce, R., & van Amerongen, H. (2013). Light-harvesting in photosystem I. *Photosynthesis Research*, *116*(2–3), 153–166.

de Bianchi, S., Betterle, N., Kouril, R., Cazzaniga, S., Boekema, E., Bassi, R., & Dall'Osto, L. (2011). Arabidopsis mutants deleted in the light-harvesting protein Lhcb4 have a disrupted photosystem II macrostructure and are defective in photoprotection. *Plant Cell*, *23*(7), 2659–2679.

Degreef, J., Butler, W. L., Roth, T. F., & Frederic, H. (1971). Control of senescence in marchantia by phytochrome. *Plant Physiology*, *48*(4), 407–412.

Dietzel, L., Brautigam, K., & Pfannschmidt, T. (2008). Photosynthetic acclimation: State transitions and adjustment of photosystem stoichiometry – Functional relationships between short-term and long-term light quality acclimation in plants. *FEBS Journal*, *275*(6), 1080–1088.

Dikaios, I., Schiphorst, C., Dall'Osto, L., Alboresi, A., Bassi, R., & Pinnola, A. (2019). Functional analysis of LHCSR1, a protein catalyzing NPQ in mosses, by heterologous expression in *Arabidopsis thaliana*. *Photosynthesis Research*, *142*(3), 249–264.

Franklin, K. A., & Quail, P. H. (2010). Phytochrome functions in Arabidopsis development. *Journal of Experimental Botany*, *61*(1), 11–24.

Fujita, Y., & Murakami, A. (1987). Regulation of electron-transport composition in cyanobacterial photosynthetic system – Stoichiometry among photosystem-I and photosystem-II complexes and their light-harvesting antennae and cytochrome-B6 cytochrome-F complex. *Plant and Cell Physiology*, *28*(8), 1547–1553.

Gan, F., Shen, G., & Bryant, D. A. (2014). Occurrence of far-red light photoacclimation (FaRLiP) in diverse cyanobacteria. *Life (Basel)*, *5*(1), 4–24.

Gan, F., Zhang, S. Y., Rockwell, N. C., Martin, S. S., Lagarias, J. C., & Bryant, D. A. (2014). Extensive remodeling of a cyanobacterial photosynthetic apparatus in far-red light. *Science*, *345*(6202), 1312–1317.

Glick, R. E., Mccauley, S. W., Gruissem, W., & Melis, A. (1986). Light quality regulates expression of chloroplast genes and assembly of photosynthetic membrane complexes. *Proceedings of the National Academy of Sciences of the United States of America*, *83*(12), 4287–4291.

Glick, R. E., Mccauley, S. W., & Melis, A. (1985). Effect of light quality on chloroplast-membrane organization and function in pea. *Planta*, *164*(4), 487–494.

Gobets, B., & van Grondelle, R. (2001). Energy transfer and trapping in photosystem I. *Biochimica et Biophysica Acta – Bioenergetics*, *1507*(1–3), 80–99.

Grebe, S., Trotta, A., Bajwa, A. A., Suorsa, M., Gollan, P. J., Jansson, S., … Aro, E. M. (2019). The unique photosynthetic apparatus of Pinaceae: Analysis of photosynthetic complexes in *Picea abies*. *Journal of Experimental Botany*, *70*(12), 3211–3225.

Heinemeyer, J., Eubel, H., Wehmhoner, D., Jansch, L., & Braun, H. P. (2004). Proteomic approach to characterize the supramolecular organization of photosystems in higher plants. *Phytochemistry*, *65*(12), 1683–1692.

Hogewoning, S. W., Wientjes, E., Douwstra, P., Trouwborst, G., van Ieperen, W., Croce, R., & Harbinson, J. (2012). Photosynthetic quantum yield dynamics: From photosystems to leaves. *Plant Cell*, *24*(5), 1921–1935.

Hu, Q., Miyashita, H., Iwasaki, I., Kurano, N., Miyachi, S., Iwaki, M., & Itoh, S. (1998). A photosystem I reaction center driven by chlorophyll *d* in oxygenic photosynthesis. *Proceedings of the National Academy of Sciences of the United States of America*, *95*(22), 13319–13323.

Jarvi, S., Suorsa, M., Paakkarinen, V., & Aro, E. M. (2011). Optimized native gel systems for separation of thylakoid protein complexes: Novel super- and mega-complexes. *Biochemical Journal*, *439*, 207–214.

Kim, J. H., Glick, R. E., & Melis, A. (1993). Dynamics of photosystem stoichiometry adjustment by light quality in chloroplasts. *Plant Physiology*, *102*(1), 181–190.

Kotabova, E., Jaresova, J., Kana, R., Sobotka, R., Bina, D., & Prasil, O. (2014). Novel type of red-shifted chlorophyll *a* antenna complex from *Chromera velia*. I. Physiological relevance and functional connection to photosystems. *Biochim Biophys Acta*, *1837*(6), 734–743.

Kotakis, C., Kyzeridou, A., & Manetas, Y. (2014). Photosynthetic electron flow during leaf senescence: Evidence for a preferential maintenance of photosystem I activity and increased cyclic electron flow. *Photosynthetica*, *52*(3), 413–420.

Kouril, R., van Oosterwijk, N., Yakushevska, A. E., & Boekema, E. J. (2005). Photosystem I: A search for green plant trimers. *Photochemical & Photobiological Sciences*, *4*(12), 1091–1094.

Laemmli, U. (1970). SDS-page Laemmli method. *Nature*, *227*, 680–685.

Lemeille, S., & Rochaix, J. D. (2010). State transitions at the crossroad of thylakoid signalling pathways. *Photosynthesis Research*, *106*(1–2), 33–46.

Li, X. P., Bjorkman, O., Shih, C., Grossman, A. R., Rosenquist, M., Jansson, S., & Niyogi, K. K. (2000). A pigment-binding protein essential for regulation of photosynthetic light harvesting. *Nature*, *403*(6768), 391–395.

Lim, J., Park, J.-H., Jung, S., Hwang, D., Nam, H. G., & Hong, S. (2018). Antagonistic roles of phyA and phyB in far-red light-dependent leaf senescence in *Arabidopsis thaliana*. *Plant and Cell Physiology*, *59*(9), 1753–1764.

Lim, P. O., Kim, H. J., & Nam, H. G. (2007). Leaf senescence. *Annual Review of Plant Biology*, *58*, 115–136.

Martinez-Garcia, J. F., Gallemi, M., Molina-Contreras, M. J., Llorente, B., Bevilaqua, M. R. R., & Quail, P. H. (2014). The shade avoidance syndrome in Arabidopsis: The antagonistic role of phytochrome A and B differentiates vegetation proximity and canopy shade. *PLoS One*, *9*(10), e109275.

Mascoli, V., Bersanini, L., & Croce, R. (2020). Far-red absorption and light-use efficiency trade-offs in chlorophyll *f* photosynthesis. *Nature Plants*, *6*(8), 1044–1053.

Mathur, S., Agrawal, D., & Jajoo, A. (2014). Photosynthesis: Response to high temperature stress. *Journal of Photochemistry and Photobiology B: Biology*, *137*, 116–126.

Melis, A., & Brown, J. S. (1980). Stoichiometry of system I and system II reaction centers and of plastoquinone in different photosynthetic membranes. *Proceedings of the National Academy of Sciences*, *77*(8), 4712–4716.

Melis, A., & Harvey, G. W. (1981). Regulation of photosystem stoichiometry, chlorophyll-A and chlorophyll-B content and relation to chloroplast ultrastructure. *Biochimica et Biophysica Acta*, *637*(1), 138–145.

Minagawa, J. (2011). State transitions—The molecular remodeling of photosynthetic supercomplexes that controls energy flow in the chloroplast. *Biochimica et Biophysica Acta (BBA) – Bioenergetics*, *1807*(8), 897–905.

Mishra, D., & Pradhan, P. (1973). Regulation of senescence in detached rice leaves by light, benzimidazole and kinetin. *Experimental Gerontology*, *8*(3), 153–155.

Mukherjee, A. (2020). State transition regulation in *Chlamydomonas reinhardtii*. *Plant Physiology*, *183*(4), 1418–1419.

Nawrocki, W. J., Santabarbara, S., Mosebach, L., Wollman, F. A., & Rappaport, F. (2016). State transitions redistribute rather than dissipate energy between the two photosystems in Chlamydomonas. *Nature Plants*, *2*, 16031.

Nicol, L., Nawrocki, W. J., & Croce, R. (2019). Disentangling the sites of non-photochemical quenching in vascular plants. *Nature Plants*, *5*(11), 1177–1183.

Nurnberg, D. J., Morton, J., Santabarbara, S., Telfer, A., Joliot, P., Antonaru, L. A., … Rutherford, A. W. (2018). Photochemistry beyond the red limit in chlorophyll *f*-containing photosystems. *Science*, *360*(6394), 1210–1213.

Ort, D. R., Merchant, S. S., Alric, J., Barkan, A., Blankenship, R. E., Bock, R., … Zhu, X. G. (2015). Redesigning photosynthesis to sustainably meet global food and bioenergy demand. *Proceedings of the National Academy of Sciences of the United States of America*, *112*(28), 8529–8536.

Peterson, R. B., & Havir, E. A. (2000). A nonphotochemical-quenching-deficient mutant of *Arabidopsis thaliana* possessing normal pigment composition and xanthophyll-cycle activity. *Planta*, *210*(2), 205–214.

Porra, R., Thompson, W., & Kriedemann, P. (1989). Determination of accurate extinction coefficients and simultaneous equations for assaying chlorophylls *a* and *b* extracted with four different solvents: Verification of the concentration of chlorophyll standards by atomic absorption spectroscopy. *Biochimica et Biophysica Acta (BBA) – Bioenergetics*, *975*(3), 384–394.

Rivadossi, A., Zucchelli, G., Garlaschi, F. M., & Jennings, R. C. (1999). The importance of PSI chlorophyll red forms in light-harvesting by leaves. *Photosynthesis Research*, *60*(2–3), 209–215.

Ruban, A. V., & Johnson, M. P. (2009). Dynamics of higher plant photosystem cross-section associated with state transitions. *Photosynthesis Research*, *99*(3), 173–183.

Santabarbara, S., Casazza, A. P., Belgio, E., Kaňa, R., & Prášil, O. (2020). Light harvesting by long-wavelength chlorophyll forms (red forms) in algae: Focus on their presence, distribution and function. *Photosynthesis in Algae: Biochemical and Physiological Mechanisms*, *45*, 261–297.

Shimakawa, G., & Miyake, C. (2019). What quantity of photosystem I is optimum for safe photosynthesis? *Plant Physiology*, *179*(4), 1479–1485.

Soulier, N., Laremore, T. N., & Bryant, D. A. (2020). Characterization of cyanobacterial allophycocyanins absorbing far-red light. *Photosynthesis Research*, *145*(3), 189–207.

Suorsa, M., Rantala, M., Danielsson, R., Jarvi, S., Paakkarinen, V., Schroder, W. P., … Aro, E. M. (2014). Dark-adapted spinach thylakoid protein heterogeneity offers insights into the photosystem II repair cycle. *Biochimica et Biophysica Acta*, *1837*(9), 1463–1471.

Takabayashi, A., Kadoya, R., Kuwano, M., Kurihara, K., Ito, H., Tanaka, R., & Tanaka, A. (2013). Protein co-migration database (PCoM-DB) for Arabidopsis thylakoids and Synechocystis cells. *Springerplus*, *2*(1), 148.

Walters, R. G., & Horton, P. (1994). Acclimation of *Arabidopsis thaliana* to the light environment: Changes in composition of the photosynthetic apparatus. *Planta*, *195*(2), 248–256.

Wientjes, E., van Amerongen, H., & Croce, R. (2013). Quantum yield of charge separation in photosystem II: Functional effect of changes in the antenna size upon light acclimation. *The Journal of Physical Chemistry B*, *117*(38), 11200–11208.

Wilhelm, C., Krámer, P., & Wild, A. (1985). Effect of different light qualities on the ultrastructure, thylakoid membrane composition and assimilation metabolism of *Chlorella fusca*. *Physiologia Plantarum*, *64*(3), 359–364.

Wolf, B. M., & Blankenship, R. E. (2019). Far-red light acclimation in diverse oxygenic photosynthetic organisms. *Photosynthesis Research*, *142*(3), 349–359.

Woo, H. R., Kim, H. J., Nam, H. G., & Lim, P. O. (2013). Plant leaf senescence and death – Regulation by multiple layers of control and implications for aging in general. *Journal of Cell Science*, *126*(Pt 21), 4823–4833.

Wood, W. H. J., MacGregor-Chatwin, C., Barnett, S. F. H., Mayneord, G. E., Huang, X., Hobbs, J. K., … Johnson, M. P. (2018). Dynamic thylakoid stacking regulates the balance between linear and cyclic photosynthetic electron transfer. *Nature Plants*, *4*(2), 116–127.

Xu, P., Tian, L., Kloz, M., & Croce, R. (2015). Molecular insights into zeaxanthin-dependent quenching in higher plants. *Scientific Reports*, *5*(1), 1–10.

SUPPORTING INFORMATION

Additional supporting information may be found online in the Supporting Information section at the end of this article.

How to cite this article: Hu C, Nawrocki WJ, Croce R. Long-term adaptation of *Arabidopsis thaliana* to far-red light. *Plant Cell Environ*. 2021;44:3002–3014. https://doi.org/10.1111/pce.14032